WOOD RESEARCH
65 (2): 2020
257-270
doi.org/10.37763/wr.1336-4561/65.2.257270

IMPACT OF ELECTRICAL CABLES EMBEDDED INTO ORIENTED STRAND BOARD ON CRITICAL HEAT FLUX

Jozef Martinka, Tomáš Štefko, Igor Wachter, Peter Rantuch
Slovak University of Technology in Bratislava
Faculty of Materials Science and Technology In Trnava
Trnava, Slovakia

(Received August 2019)

ABSTRACT

The paper deals with the research of electrical cables embedded in surface grooves of OSBs and its impact on the critical heat flux. An OSB type 3 board (structural board for use in dry or humid environments) and an electrical cable with fire reaction class $B2_{ca}$ have been investigated. Four different configurations of grooves were investigated. The first configuration consisted of an OSB without grooves (control sample). The second configuration consisted of an OSB with a single groove in the centre in which the electrical cable was mounted. In the third and fourth configurations, there were three and five grooves, respectively in which the electrical cables were mounted (the width of the grooves and the spacing between them was 9 mm). The critical heat flux was calculated from the ignition times at five different heat fluxes (30, 35, 40, 45 and 50 $kW \cdot m^{-2}$) by using a cone calorimeter. The obtained data showed that the OSB without grooves (first configuration) shows the lowest critical heat flux (8.6 $kW \cdot m^{-2}$) and the lowest standard deviation of ± 0.5 $kW \cdot m^{-2}$ (lower ignition resistance) compared to the other configurations (critical heat flux in the range from 9 to 10 $kW \cdot m^{-2}$ and standard deviation from 3.1 to 3.2 $kW \cdot m^{-2}$).

KEYWORDS: Critical heat flux, oriented strand board, electrical cables, fire investigation, fire risk, safety.

INTRODUCTION

Critical heat flux is the minimum heat flux needed to ignite a material or product. The critical heat flux is related to the time interval of its action. As the time interval increases, the critical heat flux decreases (at a longer exposure time, lower heat flux is sufficient to ignite the same material). In practice, 30 minutes time interval for the critical heat flux is most often considered, as the critical heat flux decreases only slightly with increasing time interval above the given value.

The critical heat flux is determined from the material ignition times measured at a minimum of three different heat fluxes (higher than the critical heat flux). It is necessary to identify whether the material is thermally thick or thin before determining the critical heat flux. Thermally thin material is a material which is firstly overheated throughout the cross-section and then ignited as a result of exposure to the heat flux. This means the temperature is distributed uniformly through the sample. Conversely, thermally thick material is ignited by the heat flux before it is heated over its entire cross-section to approximately the same temperature. The difference between thermally thin and thermally thick material is illustrated in Fig. 1.

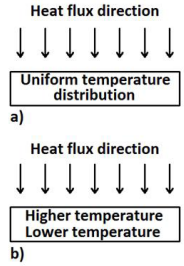

Fig. 1: Temperature distribution along cross section for a) thermally thin and b) thermally thick material.

The thermal thickness of a material depends on a large number of parameters (especially the thickness of the material, its density, thermal conductivity, specific heat capacity, and heat flux applied to the surface of the material and others). For the purposes of calculating the critical heat flux, according to Babrauskas and Parker (1987), the thermal thickness of a material can be estimated from the density of the material and the heat flux to which its surface is exposed, according to Eq. 1:

$$L = 0.6\frac{\rho}{q} \tag{1}$$

where: L is the thickness from which the material behaves as thermally thick (mm), ρ is the density of the material (kg·m^{-3}) and q is the heat flux density applied to the surface of the material (kW·m^{-2}).

The procedure for calculating the critical heat flux of materials is given in the scientific papers of Mikkola and Wichman (1989), Spearpoint and Quintiere (2001), Tewarson (2002) and Mikkola (2009). All cited methods are based on an experimental determination of material ignition time at a minimum three applied heat fluxes. The simplest method of calculation is given by Tewarson (2002), according to which the critical heat flux is calculated from the statistical dependence of the ignition time (raised to the power of -1/2) on the heat flux. Critical heat flux is then calculated from this statistical dependence (equation) by substituting 0 in the ignition time (mathematically corresponds to infinite ignition time). A more sophisticated method is given by Mikkola and Wichman (1989) and Mikkola (2009). According to the cited authors, the equation of statistical dependence differs for thermally thin and thermally thick materials. For thermally thin materials, the ignition time is raised to the power of -1 in the equation of the statistical dependence of ignition time on the heat flux. For thermally thick materials, the ignition time is raised to the power of -1/2. The critical heat flux is calculated as in the Tewarson (2002) method by substituting zero for the ignition time raised to -1/2 (thermally thick materials) or

-1 (thermally thin materials). According to the cited authors, a value of 3 kW·m^{-2} is added to the calculated value representing heat losses and the fact that the critical heat flux is not calculated for the infinite ignition time but for the ignition time of 30 minutes. According to Spearpoint and Quintiere (2001), the value calculated from the equation of statistical dependence is divided by the constant 0.76. The cited authors give a calculation procedure only for thermally thick materials.

In addition to the critical heat flux, the surface temperature at the moment of ignition is very important. Ignition temperature is calculated according to Eq. 2 reported by Spearpoint and Quintiere (2001) or Eq. 2 presented by Xu et al. (2015). Eq. 3 is a simplified form of equation (2) as it neglects heat exchange by convection.

$$q_{\mathrm{cr}} = \sigma\left(T_{\mathrm{ig}}^4 - T_0^4\right) + h_{\mathrm{c}}\left(T_{\mathrm{ig}} - T_0\right) \tag{2}$$

where: q_{cr} is critical heat flux (kW·m^{-2}), σ is the Stefan-Boltzmann constant (5.67·10^{-8} W·m^{-2}·K^{-4}), T_{ig} is ignition temperature (K), T_0 is the ambient temperature (normally assumed 293.15 K) and hc is the natural convective heat transfer coefficient (normally assumed 5 W·m^{-2}·K^{-1}).

$$T_{\mathrm{ig}} = \left(\frac{q_{\mathrm{cr}}}{\sigma}\right)^{1/4} \tag{3}$$

Ignition temperature does not coincide with flash-ignition temperature and spontaneous-ignition temperature determined according to ISO 871 (2006). These values for selected lignocellulosic materials are given in scientific papers e.g. Zachar (2010) and Zachar et al. (2012). This is due to the differences in test equipment, test procedure and method for determining ignition temperature on one hand and flash-ignition temperature or spontaneous-ignition temperature on the other hand. The advantage of ignition temperature over flash-ignition temperature or spontaneous-ignition temperature is its higher informative value for the needs of fire modelling. In addition, lignocellulosic materials can be characterized by the temperature from which they begin to thermally decompose. This temperature may be determined by thermogravimetric analysis. The thermogravimetric decomposition temperatures of selected lignocellulosic materials are shown in the scientific works of Kacik et al. (2017) and Markova et al. (2018). Other methods of assessing the fire safety of lignocellulosic materials can be found in the scientific works of Terenova et al. (2018) and Osvaldova et al. (2018).

In addition to the critical heat flux and ignition temperature, the material resistance against initiation is expressed by the Thermal Response Parameter (TRP). TRP is a very useful parameter for engineering calculations to assess resistance to ignition and fire propagation (Khan et al. 2016). TRP is defined as the resistance of a material to generate a combustible mixture (Tewarson et al. 1992, Tewarson 2002 and ASTM E2058 2002). TRP is calculated according to Eq. 4, which was used in the work of Tewarson (2002).

$$t_{\mathrm{ig}}^{-1/2} = \frac{q_{\mathrm{e}} - q_{\mathrm{cr}}}{\mathrm{TRP}} \tag{4}$$

where: t_{ig} is the ignition time (s), q_e is the heat flux applied to the surface of the material (kW·m^{-2}), q_{cr} is the critical heat flux (kW·m^{-2}) and the TRP is the thermal response parameter (kW·s$^{-1/2}$·m^{-2}).

At present, the critical heat flux, ignition temperature and thermal response parameter of all technically significant wood and lignocellulosic materials are known. However, critical heat flux

and other initiation characteristics depend on a large number of external factors. Electrical cables are often mounted on the surface or into the grooves of OSB boards. An unresolved problem is the effect of electrical cables mounted into the grooves of OSBs on the critical heat flux of the resulting configuration. In such grooves, electrical cables with a fire reaction class $B2_{ca}$ are often installed. The aim of this paper is therefore to determine the effect of the electrical cables with fire reaction class $B2_{ca}$ embedded in the surface groves of the OSB board on the ignition parameters (critical heat flux, ignition temperature and thermal response parameter).

MATERIALS AND METHODS

Materials

The effect of the electrical cable embedded in the surface grooves of the OSB on ignition parameters of resulting configuration was determined for OSB type 3 (construction board for the use in dry or wet environment) according to EN 300 (2006). Basic parameters of examined OSBs are shown in Tab. 1.

Tab. 1: Basic characteristics of investigated OSB boards.

Thickness (mm)	25.4
Density ($kg \cdot m^{-3}$)	609 ± 16
Water content (mass %)	5.1 ± 0.3
Emissivity (-)	0.89
Composition (mass %)	93.6 Coniferous wood
	4.7 Polyurethane resin
	1.7 Paraffin

The dimensions of the tested OSB samples were 100 x 100 x 25.4 mm (± 1 mm). The samples were prepared in four configurations. The first control configuration was without any grooves in the OSB surface (comparative sample). In the second configuration, there was one groove with a width and depth of 9 mm (in which one electrical cable was installed) in the centre of the OSB surface. In a third configuration, there were three grooves in the OSB surface (each 9 mm wide and deep). The first groove was positioned as in the second configuration. Position of the second and third groove was on both sides of the central groove with 9 mm spacing (from the edges of a central groove). Electrical cables were installed in all three grooves. The fourth configuration contained five grooves, with equal spacing and dimensions (9 mm). Electrical cables were installed in all grooves. The configuration of the samples is shown in Fig. 2.

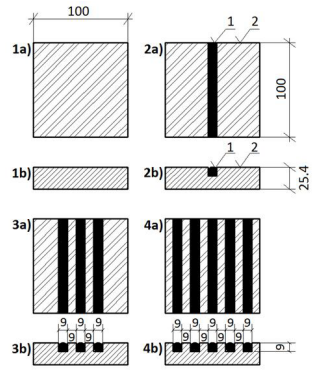

1- electrical cable, 2- OSB (dimensions in mm).

Fig. 2: Configurations of investigated samples: 1a) first configuration - view from above, 1b) first configuration - cross section, 2a) second configuration – view from above, 2b) second configuration – cross section, 3a) third configuration – view from above, 3b) third configuration – cross section, 4a) forth configuration – view from above, 4b) forth configuration – cross section.

Tested electrical cable CHKE-R J3x1.5, produced and supplied by VUKI, a.s., Bratislava, Slovakia, was installed in the grooves of the OSB boards. CHKE-R is a three-wire power cable designed for fixed installation, with flame spread resistance. The cable does not show fire circuit integrity. The electrical cable consists of three insulated electrical conductors housed inside the sheath that protect the electrical cable from external influences and its surrounding from electric shock. The space between the insulated conductors and the sheath is filled with bedding. Properties and materials of the CHKE-R cable are illustrated in Tab. 2.

Tab. 2: Basic parameters of investigated electrical cable.

Cable diameter (mm)	8.2
Insulated conductor diameter (mm)	2.6
Conductors diameter (mm)	1.38
Conductors cross section (mm^2)	1.50
Mass of copper conductors ($g \cdot m^{-1}$)	37.5
Mass of insulation ($g \cdot m^{-1}$)	17.8
Mass of bedding ($g \cdot m^{-1}$)	23.6
Mass of sheath ($g \cdot m^{-1}$)	33.2
Total mass ($g \cdot m^{-1}$)	112.1
Material of conductor (-)	Copper
Material of conductor insulation (-)	Polyethylene copolymer
Material of bedding (-)	$Al(OH)_3$ + $Mg(OH)_2$ filled polyethylene copolymer
Material of sheath (-)	$Al(OH)_3$ + $Mg(OH)_2$ filled polyethylene copolymer
Rated voltage DC (V)	1000
Rated voltage AC (V)	600
Reaction to fire class (-)	$B2_{ca}$, s1, d1, a1
Resistance to flame spread (-)	Yes
Circuit integrity during fire (-)	No

The cross-section scheme of the CHKE-R electrical cable is shown in Fig. 3.

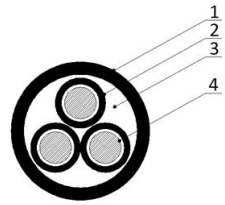

1- sheath, 2- insulation, 3- bedding, 4- copper wire.

Fig. 3: Cross section of investigated cable.

Methods

The critical heat flux was calculated from the ignition times measured at five heat fluxes (30, 35, 40, 45 and 50 kW·m^{-2}), according to Mikkola and Wichman (1989), Spearpoint and Quintiere (2001), Tewarson (2002) and Mikkola (2009). Ignition temperature was determined according to Spearpoint and Quintier (2001) and the thermal response parameter by the Tewarson (2002).

Ignition times were determined on a cone calorimeter. The cone calorimeter and test procedure are described in ISO 5660-1 (2015). Investigated heat fluxes (30, 35, 40, 45 and 50 kW·m^{-2}) and sample configurations (Fig. 2) were tested at least three times (any outlying values were discarded and the measurement was repeated). As a result, average values are reported.

The cone calorimeter and the samples after their initiation (after the determination of the ignition time) are shown in Fig. 4.

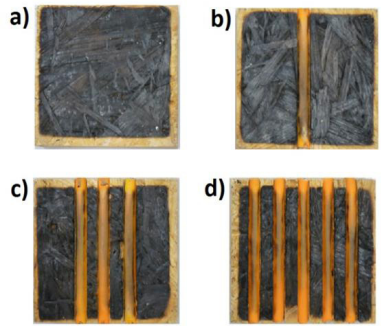

Fig. 4: Photographs of a) first configuration of sample after ignition, b) second configuration of sample after ignition, c) third configuration of sample after ignition and d) forth configuration of sample after ignition.

RESULTS AND DISCUSSION

Examined ignition times for all sample configurations and heat fluxes are shown in Tab. 3.

Tab. 3: Time to ignition of different sample configurations using heat fluxes form 30 to 50 kW·m^{-2}.

	Time to ignition (s)			
Heat flux (kW·m^{-2}) / Configuration (-)	1st	2nd	3rd	4th
30	60	67	87	67
30	67	70	66	63
30	73	69	66	74
Average time (s)	66.7 ± 5.3	68.7 ± 1.3	73 ± 9.9	68 ± 4.5
35	40	37	35	46
35	38	38	41	41
35	40	37	57	42
Average time (s)	39.3 ± 0.9	37.3 ± 0.5	44.3 ± 9.3	43 ± 2.2
40	33	30	34	30
40	40	27	41	28
40	29	26	37	33
Average time (s)	34 ± 4.5	27.7 ± 1.7	37.3 ± 2.9	30.3 ± 2.1
45	25	21	27	25
45	19	28	28	23
45	29	20	25	23
Average time (s)	24.3 ± 4.1	23 ± 3.6	26.7 ± 1.2	23.7 ± 0.9
50	19	21	22	23
50	19	16	19	13
50	19	16	21	21
Average time (s)	19 ± 0	17.7 ± 2.4	20.7 ± 1.2	19 ± 4.3

The dependence of the average initiation time (raised to the power of -1/2) on the heat flux, together with the equations of statistical dependence, are shown in Fig. 5. Critical heat fluxes calculated from the equations of statistical dependence on Fig. 5 according to Mikkola and Wichman (1989), Spearpoint and Quintiere (2001), Tewarson (2002) and Mikkola (2009) are shown in Tab. 4.

Tab. 4: Critical heat fluxes for investigated configurations.

	Critical heat flux (kW·m^{-2})			
Method (-) / Configuration (-)	1st	2nd	3rd	4th
Tewarson (2002)	5.6 ± 0.5	7 ± 3.2	6 ± 3.2	6.9 ± 3.1
Mikkola and Wichman (1989)	8.6 ± 0.5	10 ± 3.2	9 ± 3.2	9.9 ± 3.1
Spearpoint and Quintiere (2001)	7.4 ± 0.5	9.2 ± 3.2	7.9 ± 3.2	9.1 ± 3.1

According to Scudamore et al. (1991) and Tewarson (2002), the critical heat flux of most organic polymers ranges from 10 to 15 kW·m^{-2}, while the critical heat flux of most lignocellulosic materials is approximately 10 kW·m^{-2}. Similar critical heat flux values of lignocellulosic materials indicate e.g. and Martinka et al. (2017) and Martinka (2018). These values apply to lignocellulosic materials without grooves in their surface and without the installation of electrical

cables (therefore, the conditions of determination correspond to the first configuration). It follows that the critical heat fluxes of the first configuration of OSB samples calculated according to Mikkola and Wichman (1989) and Spearpoint and Quintiere (2001) are comparable to those published for lignocellulosic materials in the cited papers.

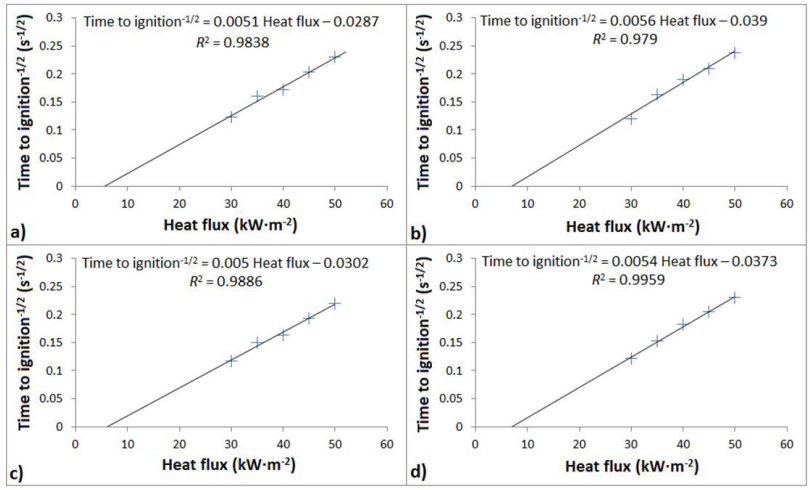

Fig. 5: Dependences of time to ignition$^{-1/2}$ on heat flux for a) first configuration, b) second configuration, c) third configuration and d) forth configuration.

The critical heat flux of halogen-free electrical cables (12 and 21 mm in diameter) is according to Meinier et al. (2018) in the range of 10.6 to 12.8 kW·m^{-2}. The cited author's team assumed that the examined electrical cables behaved like thermally thick material during the test. The polymer components of the investigated cables (Tab. 2) were mainly copolymers based on ethylene-vinyl acetate and polyethylene, the sheath was filled mainly with Al(OH)3 (the composition was therefore similar to the cables examined in the cited study). In the cited scientific paper, the critical heat flux was determined for three electrical cables placed side by side, 12 mm apart and 27 mm apart. According to Fontaine et al. (2015), the critical heat flux of electrical cables is 10.5 kW·m^{-2}. The cables examined by the cited authors were 10 mm in diameter, and the composition of the polymer components was similar to the cables in the study by Meinier et al. (2018). Rantuch et al. (2018) determined the critical heat flux of a vertically oriented self-installed electrical cable (fire response class $B2_{ca}$) in the range of 21 to 25 kW·m^{-2}. The reason for the substantially higher critical heat flux determined by Rantuch et al. (2018) as compared to Fontaine et al. (2015) and Meinier et al. (2018) is probably the fact that a single electrical cable has a significantly higher critical heat flux than multiple electrical cables of the same type installed side by side.

The critical heat fluxes in the presented paper (Tab. 4) are consistent with the results of the aforementioned papers. The lowest critical heat flux was achieved at samples of the first configuration (OSB without an installed electrical cable). Installation of electrical cables (second to fourth configurations) caused a slight increase in critical heat flow (Tab. 4). The critical heat flux of the first sample configuration is approximately consistent with the results published for lignocellulosic materials in the scientific work of Scudamore et al. (1991), Tewarson (2002),

Martinka et al. (2017) and Martinka (2018). The critical heat flux of the second, third and fourth sample configurations is lower than the critical heat flux of electrical cables as determined by Fontaine et al. (2015), Meinier et al. (2018) and Rantuch et al. (2018) and approximately the same as the critical heat flux of lignocellulosic materials published in the aforementioned works. This is probably due to the fact that the critical heat flux of a product consisting of two different materials on the surface (in this case the OSB with electrical cables mounted in grooves on the surface) is closer to the material with lower critical heat flux.

The statistical significance of the impact of the installation of electrical cables in the grooves on the OSB surface on the critical heat flux cannot be directly assessed from the critical heat flux values (the reason is that each sample configuration has only one critical heat flux and the number of data is insufficient for statistical analysis). For this reason, two-factor analysis of variance (ANOVA) with replication of ignition times was performed. The dependence of the ignition times for all four sample configurations examined (along with a 95% confidence interval) on the heat flux is shown in Fig. 6. Ignition times (at a certain heat flux) are the only input parameter for calculating the critical heat flux. However, based on the ANOVA results, only the effect of the sample configuration on the ignition time (not on the critical heat flux) can be drawn out.

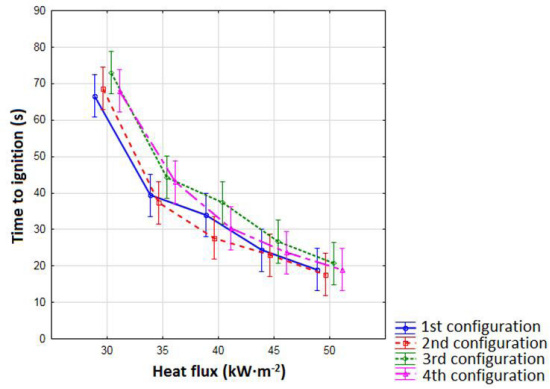

Fig. 6: Dependences of time to ignition on heat flux (with 95% confidence interval) for a) first configuration, b) second configuration, c) third configuration and d) forth configuration.

ANOVA was performed at significance level α = 0.05. The ANOVA results (p = 0.0328, F = 3.33 and Fcrit = 2.84) demonstrate that the investigated configurations show a statistically significant difference in ignition times. A post hoc Duncan´s test was performed to determine which configurations and at which heat fluxes have a statistically significant difference in ignition times. The data obtained show that there is a statistically significant difference in ignition time at a heat flux of 40 kW·m^{-2} (Duncan´s coefficient for this heat flux and sample configuration is 0.0347) between the second and third sample configurations. There is no statistically significant difference in initiation times between other sample configurations (at the same heat fluxes).

The ignition temperatures of the investigated sample configurations, calculated by the methods of Spearpoint and Quintier (2001) and Xu et al. (2015) are shown in Tab. 5. In both methods, samples of the first configuration show the lowest ignition temperature (and at the same time the lowest standard deviation). This is due to the higher resistance of electric cables (compared to OSB) to ignition.

Tab. 5: Ignition temperatures of investigated configurations.

	Ignition temperature ± SD (°C)			
Method (-) / Configuration (-)	1st	2nd	3rd	4th
Spearpoint and Quintiere	245 ± 8	341 ± 47	317 ± 52	339 ± 45
Xu et al.	328 ± 8	362 ± 48	338 ± 52	360 ± 45

Data in Tab. 5 calculated by the method of Xu et al. (2015) are consistent with data according to Janssens (1991), which for vertical oriented lignocellulosic materials reports ignition temperature in the range 314 to 394°C. Similar ignition temperature values (in the range of 306 to 372°C) of cork insulation are also reported by Rantuch et al. (2016). Different ignition temperature values of lignocellulosic materials (ranging from 456 to 488°C and for Merbau Hardwood up to 643°C) are reported by Xu et al. (2015). The cause of the substantially higher ignition temperature value determined by Xu et al. (2015) is probably the fact that the cited author's team determined the critical heat flux (input to calculate ignition temperatures) from the ignition times at heat fluxes of 25, 50 and 75 $kW \cdot m^{-2}$ (normally the critical heat flux is calculated from the ignition times measured at heat fluxes in the range of 20 to 50 $kW \cdot m^{-2}$). The ignition temperature data of the lignocellulosic material in which the electrical cable is installed have not been published in other scientific papers. Likewise, the published data on the ignition temperature of electric cables were not determined in a similar way for identical electric cables as in presented scientific paper. Gong et al. (2018) report the ignition temperature of commonly used flame retardant electrical cables (based on PVC and XLPE) in the range of 511 to 650°C. However, the cited team did not examine identical electrical cables and used a different methodology. According to Tewarson et al. (2000) and Tewarson (2002) is the ignition temperature of polyethylene (the major component of the polymer of the investigated cables) in the range 377 to 443°C. A comparison of the above data demonstrates that lignocellulosic materials have a lower ignition temperature than electrical cables with polyethylene-based polymer components. Data in Tab. 5 are consistent with this conclusion drawn from the data in the cited scientific papers (the ignition temperature of the second to fourth sample configurations is higher than the ignition temperature of the first (control) sample configuration due to the increasing proportion of electrical cables on the OSB surface).

The thermal response parameters (TRP) of the sample configurations are shown in Tab. 6. Tab. 6 show that TRP decreases with increasing heat flux. This trend is already apparent from Eq. 4. The average TRP of the first sample configuration is higher than the second sample configuration, while lower than the third sample configuration (Tab. 6). This trend can be explained by the fact that installing a cable in the surface of the OSB (creating grooves) will cause the surface to break and consequently reduce the resistance to ignition. On the other hand, the electrical cable (fire reaction class $B2_{ca}$) has, according to Rantuch et al. (2018) significantly higher critical heat flux than OSB. Thus, in the second configuration (one groove), the negative effect (surface disruption) probably prevailed over the positive effect (presence of the element - cable with a higher critical heat flux), since the ratio of the installed electrical cable surface to OSB board surface was too low. In the third configuration, the effect was reversed.

Tab. 6: Thermal response parameters for investigated configurations.

	Thermal response parameter ($kW \cdot s^{-1/2} \cdot m^{-2}$)			
Heat flux ($kW \cdot m^{-2}$) / Configuration (-)	1st	2nd	3rd	4th
30	344	352	410	353
30	363	360	357	342
30	379	357	357	371
Average TRP ($kW \cdot s^{-1/2} \cdot m^{-2}$)	362 ± 14	356 ± 3	375 ± 25	355 ± 12
35	281	262	260	292
35	274	265	282	276
35	281	262	332	279
Average TRP ($kW \cdot s^{-1/2} \cdot m^{-2}$)	279 ± 3	263 ± 1	291 ± 30	282 ± 7
40	255	236	257	236
40	281	223	282	228
40	239	219	268	248
Average TRP ($kW \cdot s^{-1/2} \cdot m^{-2}$)	258 ± 17	226 ± 7	269 ± 10	237 ± 8
45	222	197	229	216
45	194	228	233	207
45	239	192	220	207
Average TRP ($kW \cdot s^{-1/2} \cdot m^{-2}$)	218 ± 19	206 ± 16	227 ± 5	210 ± 4
50	194	197	206	207
50	194	172	192	155
50	194	172	202	198
Average TRP ($kW \cdot s^{-1/2} \cdot m^{-2}$)	194 ± 0	180 ± 12	200 ± 6	187 ± 23

For comparison, according to Scudamore et al. (1991) and Tewarson (2002) wood materials show (without flame retardant) TRP in the range from 134 to 138 $kW \cdot s^{-1/2} \cdot m^{-2}$ (flame retardant can increase this value by more than 100 $kW \cdot s^{-1/2} \cdot m^{-2}$) and polyethylene-based polymers have reached 224 - 321 $kW \cdot s^{-1/2} \cdot m^{-2}$. According to the cited authors power electrical cables (consisting of polymer components based on polyethylene and PVC) show TRP in the range of 221 - 263 $kW \cdot s^{-1/2} \cdot m^{-2}$. It should be noted that TRP was determined by the authors on a Fire Propagation Apparatus according to then applicable ASTM E2058 (2002) and only for a narrow group of tree species. However, the cited data show that the TRP of wood and wood-based materials and electrical cables are approximately in the same interval. The obtained data (Tab. 6) are in approximate conformity with the cited papers. Despite the fact that the differences in TRP between the different configurations are measurable (Tab. 6), these differences are practically negligible.

CONCLUSIONS

The impact of the electrical cables with fire reaction class $B2_{ca}$ mounted into the grooves of OSBs surface on the critical heat flux, ignition temperature and thermal response parameters was studied in this paper. The measurements were conducted on samples with 3 different configurations (OSB with 1, 3 and 5 electrical cables mounted into grooves) and on a control sample (OSB without an electrical cable).

The obtained data showed that the configuration without any electrical cable had a lower critical heat flux (8.6 ± 0.5 $kW \cdot m^{-2}$) and lower ignition temperature (328 ± 8°C) compared to

OSBs with electrical cables mounted into the grooves (critical heat flux was determined in the range from 9 to 10 $kW \cdot m^{-2}$ and ignition temperature in the range from 338 to 362°C). The effect of electrical cables mounted into the grooves of OSB boards on the TRP is not clear.

Electrical cables (fire reaction class $B2_{ca}$) mounted into grooves in the surface of the OSB boards caused a measurable increase in both critical heat flux and ignition temperature. However, this increase is negligible from a practical point of view. Therefore, on the basis of the obtained data, it can be concluded that the installation of electrical cables with the specified reaction to fire class into the OSB grooves will not cause a significant change in its tendency to ignite by thermal radiation. This conclusion applies to the experimental conditions described in this scientific work.

ACKNOWLEDGEMENTS

This work was supported by the Slovak Research and Development Agency under the contract No. APVV-16-0223.

REFERENCES

1. ASTM E2058, 2002: Standard test methods for measurement of synthetic polymer material flammability using a fire propagation apparatus.
2. Babrauskas, V., Parker, W.J., 1987: Ignitability measurements with the cone calorimeter. Fire and Materials 11(1): 31-43.
3. EN 300, 2006: Oriented strand boards (OSB). Definitions, classification and specifications.
4. Fontaine, G., Ngohang, F.E., Gay, L., Bourbigot, S., 2015: Investigation of the contribution to fire of electrical cable by a revisited mass loss cone. In: Fire Science and Technology (ed. Harada K, Matsuyama K, Himoto K, Nakamura Y, Wakatsuki K). Singapore. Springer, Pp 687-693.
5. Gong, T., Xie, Q., Huang, X., 2018: Fire behaviors of flame-retardant cables part I: Decomposition, swelling and spontaneous ignition. Fire Safety Journal 95(1): 113-121.
6. ISO 5660-1, 2015: Reaction to fire tests. Heat release, smoke production and mass loss rate. Part 1: Heat release rate (cone calorimeter method) and smoke production rate (dynamic measurement).
7. ISO 871, 2006: Plastics. Determination of ignition temperature using a hot-air furnace.
8. Janssens, M.L., 2003: Improved method for analyzing ignition data from the cone calorimeter in the vertical orientation. In: Fire Safety Science (ed. Evans DD). International Assotiation for Fire Safety Science. London. Pp 803-814.
9. Kacik, F., Luptakova, J., Smira, P., Estokova, A., Kacikova, D., Nasswettrova, A., Bubenikova, T., 2017: Thermal analysis of heat-treated silver fir wood and larval frass. Journal of Thermal Analysis and Calorimetry 130(2): 755-762.
10. Khan, M.M., Tewarson, A., Chaos, M., 2016: Combustion characteristics of materials and generation of fire products. In: SFPE Handbook of Fire Protection Engineering (ed. Hurley MJ). Pp 1143-1232, Springer, London. Pp 1143-1232.
11. Markova, I., Hroncova, E., Tomaskin, J., Turekova, I., 2018: Thermal analysis of granulometry selected wood dust particles. BioResources 13(4): 8041-8060.
12. Martinka, J., 2018: Fire risk of materials and combustible liquids. Ales Cenek Publishing House. Plzen, 142 pp.

13. Martinka, J., Hroncova, E., Kacikova, D., Rantuch, P., Balog, K., Ladomersky, J., 2017: Ignition parameters of poplar wood. *Acta Facultatis* Xylologiae Zvolen 59(1): 85-95.
14. Meinier, R., Sonnier, R., Zavaleta, P., Suard, S., Ferry, L., 2018: Fire behavior of halogen-free flame retardant electrical cables with the cone calorimeter. Journal of Hazardous Materials 342(1): 306-316.
15. Mikkola, E., 2009: Ignitability of solid materials. In: Heat Release in Fires (ed. Babrauskas V, Grayson SJ). Interscience Communications. London. Pp 225-232.
16. Mikkola E., Wichman, I.S., 1989: On the thermal ignition of combustible materials. Fire and Materials 14(3): 87-96.
17. Osvaldova, L.M., Gasparik, M., Castellanos, J.R.S., Markert, F., Kadlicova, P., Cekovska, H., 2018: Effect of thermal treatment on selected fire safety features of tropical wood. Communications - Scientific Letters of the University of Zilina 20(2): 3-7.
18. Rantuch, P., Hrusovsky, I., Martinka, J., Balog, K., 2016: Determination of the critical heat flux and the corresponding surface ignition temperature of the expanded cork plates. In: Conference proceedings of 8th International Scientific Conference Wood and Fire Safety 2016. Vol. 1, University of Zilina. Zilina. Pp 261-268.
19. Rantuch, P., Stefko, T., Martinka, J., Wachter, I., Kobeticova, H., 2018: Impact of initiator placement on ignition of the vertically positioned electrical cable. In: Conference proceedings of 18th International Multidisciplinary Scientific Conference SGEM 2018 (Vol. 18). STEF92 Technology. Sofia. Pp 419-426.
20. Scudamore, M.J., Briggs, P.J., Prager, F.H., 1991: Cone calorimetry – a review of tests carried out on plastics for the association of plastics manufacturers in Europe. Fire and Materials 15(2): 65-84.
21. Spearpoint, M.J., Quintiere, J.G., 2001: Predicting the piloted ignition of wood in the cone calorimeter using an integral model - effect of species, grain orientation and heat flux. Fire Safety Journal 36(4): 391-415.
22. Terenova, L., Dubravska, K., Majlingova, A., 2018: The impact of geometric shape of the log wall construction elements on their fire behaviour. Wood Research 63(4): 547-558.
23. Tewarson, A., 2002: Generation of heat and chemical compounds in fires. In: The SFPE Handbook of Fire Protection Engineering (ed. DiNenno PJ). National Fire Protection Association. Quincy. Pp 618-697.
24. Tewarson, A., Abu-isa, I.A., Cummings, D.R., Ladue, D.E., 2000: Characterization of the ignition behaviour of polymers commonly used in the automotive industry. In: Fire Safety Science (ed. Curtat M). International Assotiation for Fire Safety Science. London. Pp 991-1002.
25. Tewarson, A., Ogden, S.D., 1992: Fire behavior of polymethylmethacrylate. Combustion and Flame (89)3: 237-259.
26. Xu, Q., Chen, L., Harries, K.A., Zhang, F., Liu, Q., Feng, J., 2015: Combustion and charring properties of five common constructional wood species from cone calorimeter tests. Construction and Building Materials 96(1): 416-427.
27. Zachar, M., 2010: Selected deciduous wood species flash ignition and ignition temperature determination. In: Fire Engineering (ed. Mrackova E, Markova I). Technical University in Zvolen. Zvolen. Pp 431-438.
28. Zachar, M., Mitterova, I., Xu, Q., Majlingova, A., Cong, J., Galla, S., 2012: Determination of fire and burning properties of spruce wood. Drvna Industrija 63(3): 217-223.

*Jozef Martinka, Tomáš Štefko, Igor Wachter, Peter Rantuch
Slovak University of Technology in Bratislava
Faculty of Materials Science and Technology in Trnava
Jana Bottu 2781/25
917 24 Trnava
Slovakia
*Corresponding author: jozef.martinka@stuba.sk